J. Fluid Mech. (1979), *vol.* 91, *part* 1, *pp.* 111–130
Printed in Great Britain

Measurements of the growth rate and structure in plane turbulent mixing layers

By N. K. PUI† AND I. S. GARTSHORE
Department of Mechanical Engineering, University of British Columbia, Vancouver, Canada

(Received 13 September 1977 and in revised form 8 June 1978)

Mean velocity and turbulent intensity measurements are reported for five different plane turbulent mixing layers, each with a different velocity ratio. These experiments confirm that increasing free-stream turbulence causes increases in the growth rate and in the Reynolds stresses. Cross-correlation measurements with time delay made in the mixing layer with the lowest free-stream turbulence level show that the large-eddy structure had length scales in the two cross-stream directions which were roughly equal, unlike the results reported by Brown & Roshko (1974) and others. Further measurements showed that a vortex-street wake existed immediately downstream of the splitter plate and that transition occurred in the wake flow rather than in a normal laminar mixing layer. This is thought to have prevented the Brown–Roshko structures from forming. Comparison of the growth rate observed in this case with other measured results suggests that the essential or effective turbulent structure in mixing layers is independent both of velocity ratio and of the degree of two-dimensionality which exists in the largest scales of turbulence.

1. Introduction

The turbulent plane mixing layer which forms between two parallel uniform streams has for some time been grouped with jets and wakes as one of the simplest free shear flows. Its linear growth rate was thought to depend only on the ratio of the streaming velocities on each side; its structure, as indicated by non-dimensional flow constants, was apparently independent of even the bounding velocity ratio (see Townsend 1976; Sabin 1965). Recently, however, the sensitivity of mixing layers to small changes in initial conditions or free-stream turbulence levels has become evident (Rodi 1975, Batt 1975; Oster, Wygnanski & Fiedler 1976). In addition, the two-dimensional large structure first observed by Brown & Roshko (1974) is thought by some to be of fundamental importance (Roshko 1976; Dimotakis & Brown 1976) and by others to be a relic of transition (Bradshaw 1976), so that uncertainty about the turbulent structure exists.

The experiments reported here confirm the importance of free-stream turbulence but they show that the two-dimensionality of the large-eddy structure is not necessary for a well-behaved mixing layer with a normal growth rate. Apparently then, while there is still a need to quantify and explain the way in which free-stream turbulence affects mixing layers (and this is true of all turbulent shear flows) there need be less concern about the possibility that more than one type of essential turbulence structure

† Present address: Dome Petroleum Company, Calgary, Canada.

0022-1120/79/4158-5800 $02.00

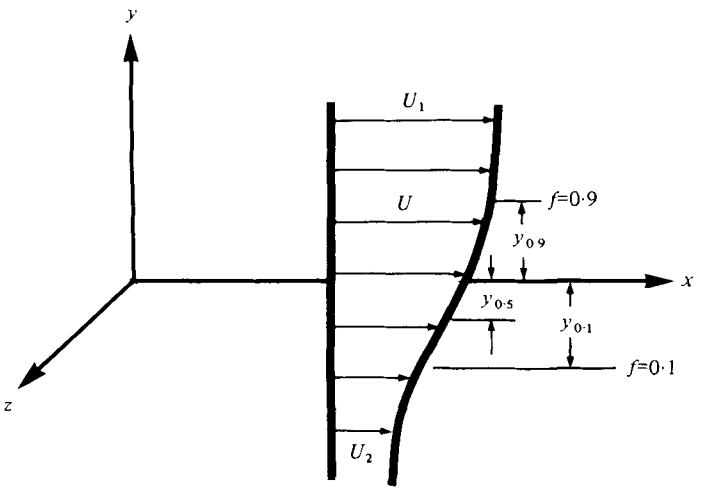

FIGURE 1. Axes used to describe mixing-layer velocities.

(two-dimensional as opposed to three-dimensional) must be understood to unscramble the turbulent shear flow puzzle. The present experiments also support earlier suggestions that the flow constants for mixing layers are, within a certain measure of uncertainty arising from initial conditions and free-stream turbulence, essentially independent of the ratio of the velocities on either side of the layer.

Early measurements made in 1969 by Pui are first reported. His experimental arrangements were such that the free-stream turbulence intensities were rather large. Later measurements with different arrangements were made specifically to investigate the effect of free-stream turbulence of small scale. Finally tests were undertaken to study the structure of the largest eddies in the flow.

It is convenient here to introduce the mathematical description of a two-dimensional shear layer that will be used hereafter. Following Townsend (1976, p. 327), we assume that the mean flow is parallel to the x, y plane, where U approaches U_1 for large positive y and U approaches U_2 for large negative y. Axes are so chosen that $V = 0$ along $y = 0$. If $U_0 \equiv U_1 - U_2$ then we assume $U_1 > U_2$ and

$$U = U_2 + U_0 f(\eta), \quad \overline{uv} = U_0^2 g(\eta), \tag{1}$$

with similar expressions for the normal Reynolds stresses, where

$$\eta \equiv (y - y_{0\cdot5})/L_0$$

and $L_0 \equiv y_{0\cdot9} - y_{0\cdot1}$ is a measure of the width of the shear layer. The quantities $y_{0\cdot9}$, $y_{0\cdot1}$ and $y_{0\cdot5}$ refer to values of y at which the function $f(\eta)$ is equal to 0·9, 0·1 or 0·5 as sketched in figure 1.

An alternative and often preferable definition of shear-layer width is the inverse of the maximum velocity derivative, i.e. a width l can be defined such that

$$l \equiv U_0 \{\partial U/\partial y\}_{\max}^{-1}.$$

If one assumes that Görtler's constant eddy viscosity approximate solution is a

reasonable description of the mean velocity profile (see, for example, Schlichting 1969, p. 598), then

$$\frac{U}{U_1} = \frac{U_2}{U_1} + \frac{1-U_2/U_1}{2}(1+\operatorname{erf}\zeta), \tag{2}$$

where $$\zeta = \sigma(y-y_{0\cdot5})/(x+x_0),$$

x_0 being a virtual origin, and

$$\operatorname{erf}\zeta \equiv \frac{2}{\sqrt{\pi}}\int_0^{\zeta} \exp(-t^2)\,dt.$$

The free constant σ and widths l and L_0 are related once the velocity profile is defined, and using (2),

$$\frac{1}{\sigma} = \frac{U_0}{2(x+x_0)}\left(\frac{\partial U}{\partial y}\right)^{-1}_{\max} \simeq 0\cdot552\frac{dL_0}{dx}.$$

Since dL_0/dx is equivalent to $L_0/(x+x_0)$ this can be written as

$$l = 1\cdot10L_0 = 2\sigma^{-1}(x+x_0). \tag{3}$$

In all cases in this investigation, the shear-layer width l was determined directly from measured velocity profile gradients; other width scales such as L_0 or σ were then determined from (3).

If the function $g(\eta)$ in (1) is independent of U_2/U_1, as Townsend argues, then

$$\frac{dl}{dx} \propto \frac{dL_0}{dx} \propto \frac{1}{\sigma} \propto \frac{1-U_2/U_1}{1+U_2/U_1}. \tag{4}$$

The relationship between shear stress and mean velocity implied by the conservation of momentum has been given by Rodi (1975) and by Townsend (1976). It is useful to show that the maximum shear stress, which can be found by differentiating this general relationship between $g(\eta)$, $f(\eta)$ and U_2/U_1 and setting $g'(\eta)$ to zero, is

$$g(\eta_m) = -\frac{dL_0}{dx}\left\{\frac{U_2}{U_0}\int_{-\infty}^{\eta_m} f\,d\eta + \int_{-\infty}^{\eta_m} f^2\,d\eta\right\}, \tag{5}$$

where η_m identifies the point at which $g(\eta)$ is a maximum, and incidentally at which $V = 0$ as well. Townsend (1976) has evaluated the integrals in (5) using the error-integral approximation to the velocity profile and taking into account the variation of η_m with U_2/U_0. His result in the present notation is

$$\frac{U_2}{U_0}\int_{-\infty}^{\eta_m} f\,d\eta + \int_{-\infty}^{\eta_m} f^2\,d\eta \simeq 0\cdot156\left\{\frac{U_2}{U_0}+\frac{1}{2}\right\},$$

so that

$$g(\eta_m) = -(0\cdot156)\frac{dL_0}{dx}\left\{\frac{U_2}{U_0}+\frac{1}{2}\right\}. \tag{6}$$

This simple relation is useful in checking measured values of the shear stress and growth rate against each other for various velocity ratios.

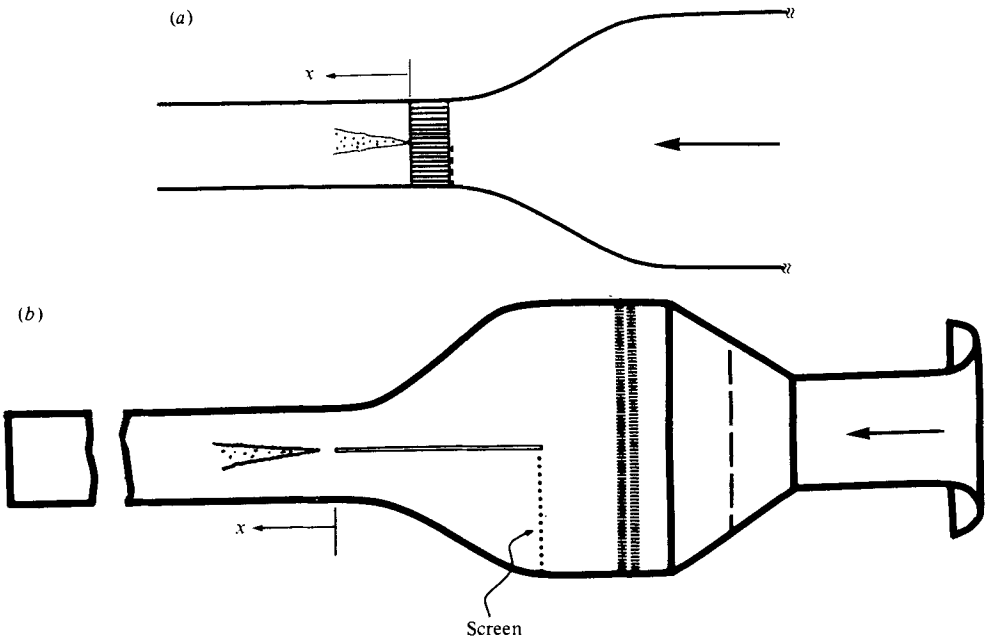

FIGURE 2. Experimental arrangement used for (*a*) tests I and (*b*) tests II.

2. Experimental arrangements

2.1. *Initial tests* (*I*)

Three mixing layers with velocity ratios of 0·65, 0·75 and 0·81 were examined initially by Pui. The measurements were made in a low-speed, closed-circuit wind tunnel with a test section 36 in. by 27 in. and 104 in. long. Boundary-layer growth in the test section is offset by four tapered corner fillets and a breather slot following the test section maintains it at atmospheric pressure.

In order to generate a mixing layer, a deep-cell honeycomb was placed at the upstream end of the test section, and a piece of screen was fastened over half of the honeycomb on the upstream side as sketched in figure 2(*a*). The honeycomb was 12 in. deep with $\frac{1}{8}$ in. hexagonal cells and a cell wall thickness of 0·0007 in. Various screen mesh sizes were used to produce the three different velocity ratios. Suitable traversing gear held the Pitot-static tubes and linearized hot wires used to make the measurements.

The honeycomb does generate turbulence in the free streams; the larger longitudinal intensity (in the higher-velocity stream) at the first measuring station, 20 in. downstream of the honeycomb exit, was about 1 %, decreasing to 0·5 % at the furthest downstream station. The larger free-stream velocity in these experiments was about 23 ft/s for all velocity ratios studied. Further details may be obtained from the thesis by Pui (1969).

2.2. *Later tests* (*II*)

The second set of experiments were made in a smaller open-circuit blower-type wind tunnel. The test section is 16 in. wide, 10 in. high at its entrance and 110 in. long. The working-section roof was adjusted to maintain atmospheric pressure all along the section length. The 4 : 1 contraction was divided in half horizontally by a $\frac{1}{16}$ in.

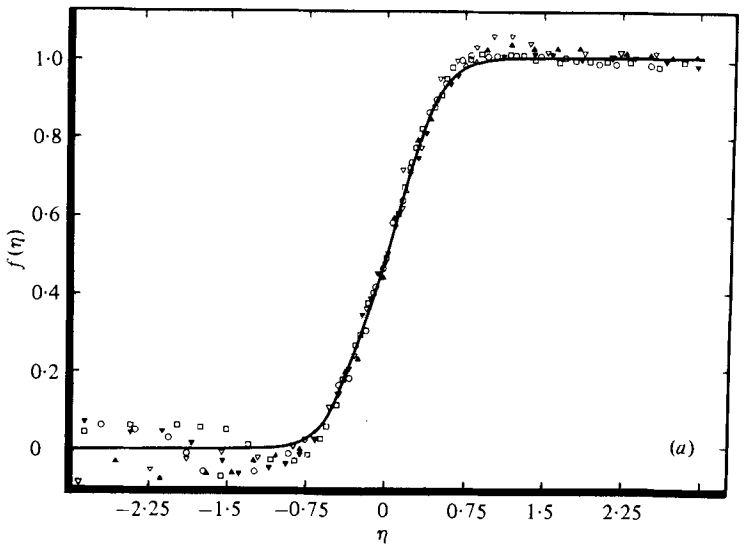

FIGURE 3*a*. For legend see p. 117.

aluminium plate and screens fastened over the lower half of the tunnel at the upstream end of the plate lowered the velocity below the plate and created the mixing layer. This arrangement is sketched in figure 2(*b*). The boundary layers leaving the plate were laminar at the speeds used, about 21 ft/s in the higher-velocity stream.

Preliminary tests showed that a significant frequency of about 30 Hz could be easily excited in the mixing layer, from a very slight vibration of the dividing plate. This oscillation was particularly noticeable in the correlation measurements described later, and is discussed in § 4. It was virtually eliminated by restraining the dividing plate with three vertical fine wires and by reducing the fan vibration to a very low level. Care was taken to make measurements in the mixing layer outside the wakes of the vertical wires restraining the dividing plate.

The mixing layer's velocity ratio U_2/U_1 was 0·83, with free-stream turbulence of between 0·1 and 0·2 %. Additional comments are made on these values in § 3.2. The turbulence intensity was increased, for later tests, by placing honeycomb pieces above and below the dividing plate close to its trailing edge. The presence of these pieces, 6 in. deep (in the x direction) and with $\frac{3}{8}$ in. cells, increased the free-stream turbulence to about 1 % and reduced the velocity ratio to 0·77.

Traverses across the flow were made in this case by a stepper motor driving a DISA traverse mechanism holding a linearized hot wire. Some results were plotted automatically after suitable analog treatment. Cross-correlations with time delay were made using a PAR correlator. Spectra were measured with an analog spectral analysis unit.

3. Discussion of results

3.1. *Tests I*

A typical mean velocity profile obtained for one velocity ratio is plotted in figure 3(*a*); corresponding turbulence intensities are given in figures 3(*b*), (*c*) and (*d*). The spreading rates were found to be linear (figure 3*e*) and these together with the consistent Reynolds-

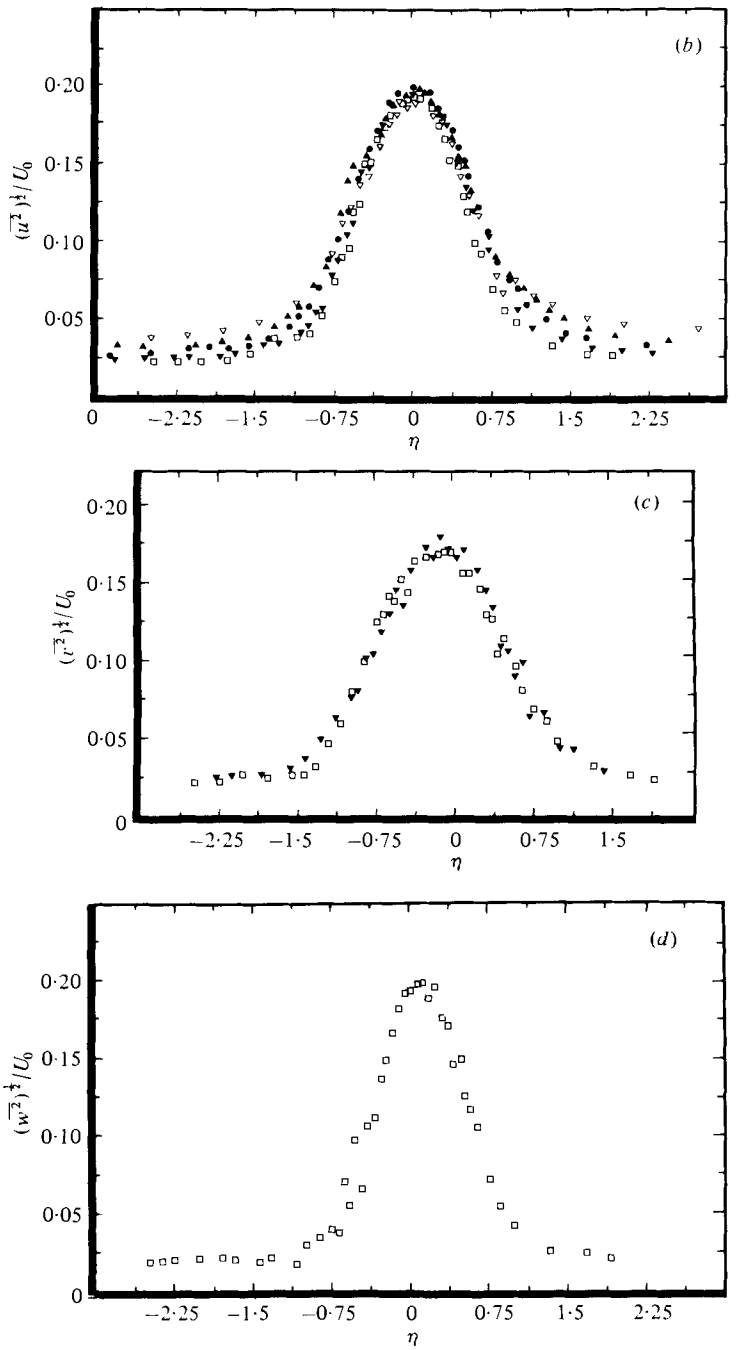

FIGURE 3*b*, *c*, *d*. For legend see p. 117.

stress profiles indicate a close approach to self-preservation. The shear stress measured at two stations with inclined wires is shown in figure 3(*f*). The maximum measured shear stress is compared with that from (6) in table 1, where a summary of all data for tests I is given. The measured shear stresses are in reasonable agreement for the lower two velocity ratios (0·65 and 0·75). For the 0·81 case, a cross-wire was used and thermal

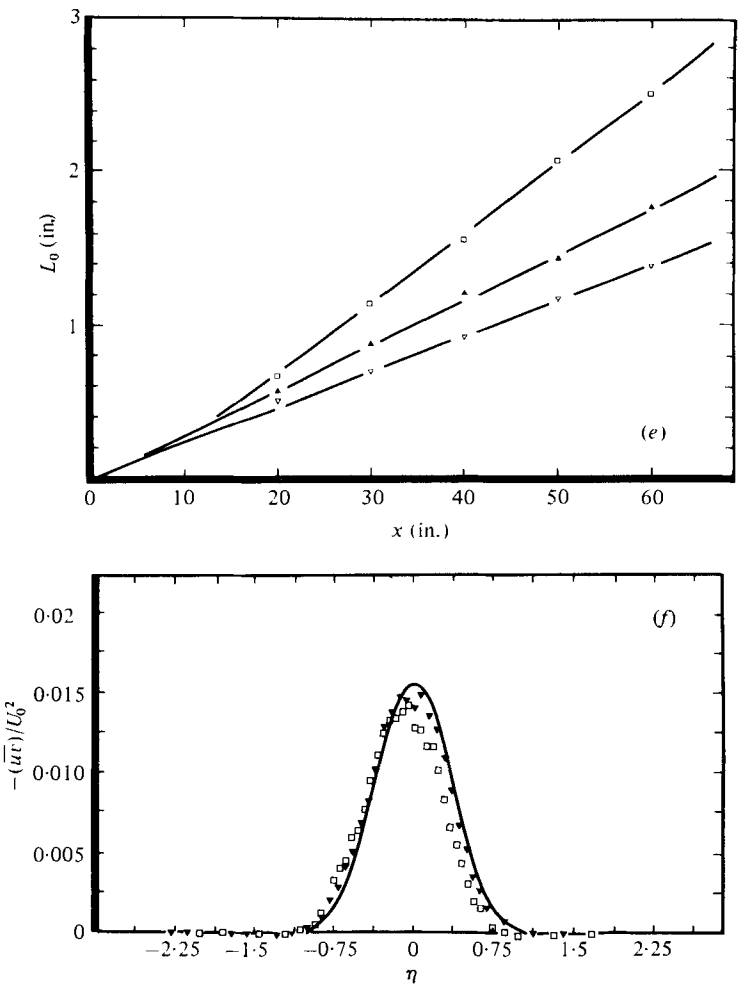

FIGURE 3. (*a*) Typical mean velocity distribution, (*b*) longitudinal turbulence intensity, (*c*) cross-stream turbulence intensity, (*d*) lateral turbulence intensity, (*e*) mixing-layer width and (*f*) shear stress from tests 1. (*a*)–(*d*), (*f*) $U_2/U_1 = 0{\cdot}75$. (*e*) ▽, $U_2/U_1 = 0{\cdot}81$; ▲, $U_2/U_1 = 0{\cdot}75$; □, $U_2/U_1 = 0{\cdot}65$. (*a*)–(*d*), (*f*) ▽, $x = 20$ in.; ▲, $x = 30$ in.; ○, $x = 40$ in.; ▼, $x = 50$ in.; □, $x = 60$ in. (*a*) ——, fitted curve. (*f*) ——, computed from velocity profile and measured growth rate.

interference between the wires is thought to be responsible for the inaccuracies of measurement. For this reason the lateral intensity is probably high in this case ($U_2/U_1 = 0{\cdot}81$) as well, but the longitudinal intensity and growth rates are thought to be accurate.

These initial results for the growth rate, turbulence kinetic energy and shear stress are compared by Rodi with other measurements. There is considerable scatter in the growth rates reported by Rodi and no definite conclusion can be drawn about the validity of (4). The longitudinal intensities for tests I listed in table 1 suggest that increasing velocity ratios U_2/U_1 produce increases in the non-dimensional stresses, a trend which would imply a change in turbulent structure with changing velocity ratio. This is not consistent with current views of the mixing layer such as that of Townsend for example (see Townsend 1976, pp. 227–230). As suggested by Patel (1973) and by

Test number	I			II(*a*)	II(*b*)
U_2/U_0	1·86	3·00	4·26	4·88	3·54
U_2/U_1	0·65	0·75	0·81	0·83	0·77
dL_0/dx	0·0421	0·0297	0·0203	0·0150	0·0280
$100[\overline{(u^2)}^{\frac{1}{2}}/U_1]_{\eta\to+\infty}$	0·9	0·9	0·8	0·2	1 to 1·3
$(-\overline{uv}/U_0^2)\times 100$ (measured)	1·67	1·46	1·85	1·22	—
$(-\overline{uv}/U_0^2)\times 100$ [from (6)]	1·54	1·62	1·51	1·25	—
$\frac{1}{0\cdot16}\frac{dL_0}{dx}\left(\frac{1+U_2/U_1}{1-U_2/U_1}\right)$	1·23	1·30	1·21	1·01	1·37
$[\overline{(u^2)}^{\frac{1}{2}}/U_0]_{\max}$	0·187	0·192	0·195	0·177	0·225
$[\overline{(v^2)}^{\frac{1}{2}}/U_0]_{\max}$	0·17	0·17	0·21	0·14	—
$[\overline{(w^2)}^{\frac{1}{2}}/U_0]_{\max}$	—	0·20	—	—	—

TABLE 1. Summary of present measurements.

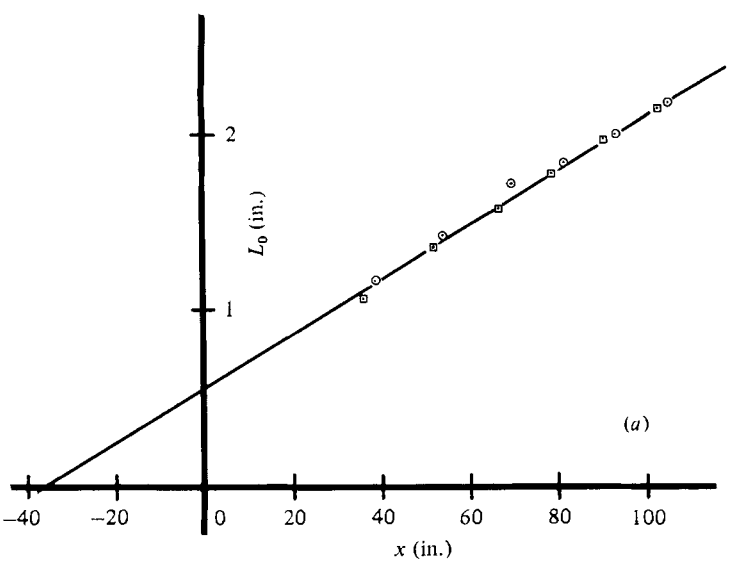

FIGURE 4*a*. For legend see p. 120.

Rodi (1975), free-stream turbulence may effect these flows increasingly as U_2/U_1 is increased, and may therefore be responsible for the apparent trend. The results described next were obtained to examine this possibility.

3.2. *Tests II*

Because the free-stream turbulence intensity was fairly high (up to 1 %) in the tests described already, and because it could not be lowered easily, a new experimental arrangement was required to examine the effect of this parameter. Large U_2/U_1 ratios were thought to be most susceptible to this effect and values of this ratio near 0·8 were found to be convenient.

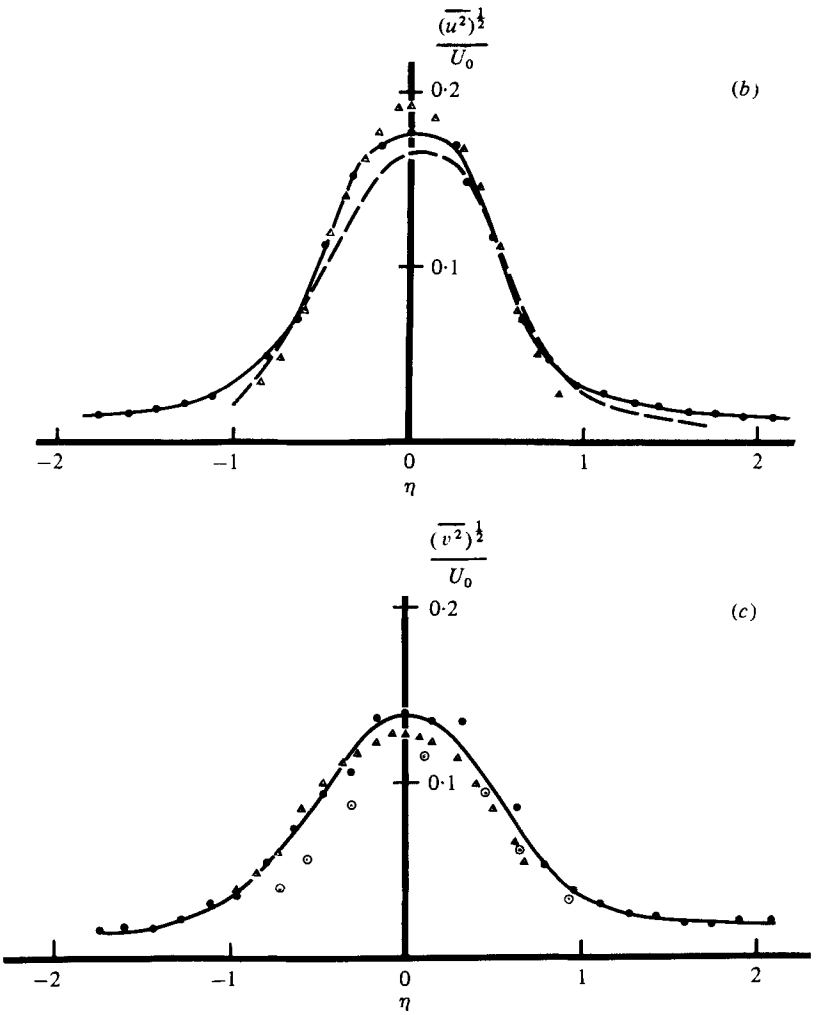

FIGURE 4*b*, *c*. For legend see p. 120.

The first 'low turbulence level' mixing layer had a velocity ratio of 0·83 and free-stream turbulence levels of between 0·12 % and 0·18 % based on the local mean velocity. The measured growth rate, maximum longitudinal intensity and maximum shear stress are listed in table 1 (results II*a*) along with the maximum shear stress calculated from (6). Shear-layer widths L_0 are shown in figure 4(*a*) and the linearity of growth together with the close agreement between the measured and calculated shear stress are reassuring checks on the measurement accuracy and development. Normal intensity profiles also collapsed satisfactorily over the last few feet of stream-wise length, so that the layer is apparently self-preserving. Typical normal and shear stress distributions are shown in figures 4(*b*), (*c*) and (*d*) for $x = 66$ in.

The Reynolds stresses in this experiment are significantly lower than comparable quantities measured in the earlier experiments I. The maximum value of $(\overline{u^2})^{\frac{1}{2}}/U_0$ of 0·177 found here is similar to other recently measured values: intensity distributions reported for $U_2 = 0$ by Champagne, Pao & Wygnanski (1976) and for $U_2 = 0{\cdot}3$ by

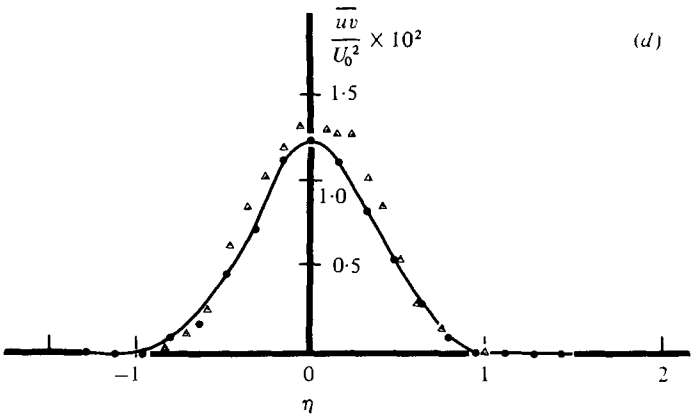

FIGURE 4. (*a*) Width, (*b*) longitudinal intensity, (*c*) cross-stream intensity and (*d*) shear stress from tests II(*a*). (*b*)–(*d*) ——, ●, present results; – – –, ○, Champagne *et al.* (1976); △, Spencer & Jones (1971).

Spencer & Jones (1971) are included in the figures for comparison. The differences in $\overline{v^2}$ on the low-velocity side ($\eta < 0$) are surprising and may reflect difficulties of measurement in a flow for which U_2 is zero.

The measured maximum value of $\overline{uv}/U_0^2$ is significantly smaller than those of experiments I and is comparable to the lowest realistic values reported for any velocity ratio. As noted by Rodi, and others, the shear stresses measured by Liepmann & Laufer (1947) and by Wygnanski & Fiedler (1970) are both unrealistically low (by over 30 %) when compared with that calculated from (6) using the observed growth rates.

The growth rate of this 'low turbulence' case is closely compatible with the constant-structure model of (4) if Liepmann & Laufer's growth rate for $U_2 = 0$ is accepted as correct. Using (4) and $dL_0/dx = 0{\cdot}16$ for $U_2 = 0$, the growth rate for a mixing layer of velocity ratio 0·83 according to (4) should be 0·015. This, to a fortuitous accuracy, is the value found in the present experiments. In any case, it now appears that the constant-structure model of the shear layer, in which the non-dimensional Reynolds stresses are independent of the velocity ratio, is at least an adequate description of overall mixing-layer behaviour provided that the flow is self-preserving and provided that the free-stream turbulence levels are sufficiently low.

Two additional comments on the present 'low turbulence' case should be made. First, the measured free-stream values of $(\overline{u^2})^{\frac{1}{2}}/U$ apparently increased in the streamwise direction, starting at 0·12 % (in the higher-velocity stream) and reaching nearly 0·5 % at the furthest downstream station. This increase was due to the proximity of the developing shear layer to the roof of the wind tunnel, on which a turbulent boundary layer was growing. The mixing layer and the boundary layer both create irrotational fluctuations outside their vortical turbulent regions, and these fluctuations extend outwards for a distance comparable to the largest lateral length scale of the turbulence, roughly equal to the shear-layer width. The irrotational velocities $\overline{u_I^2}$ decay like $(y - y_I)^{-4}$, where $y - y_I$ is the distance from the mean location of the bounding interface, as shown by Phillips (1955).

In the present experiment, the irrotational regions apparently overlap or 'time share' in the sense described by Dean & Bradshaw (1976), creating a minimum in the

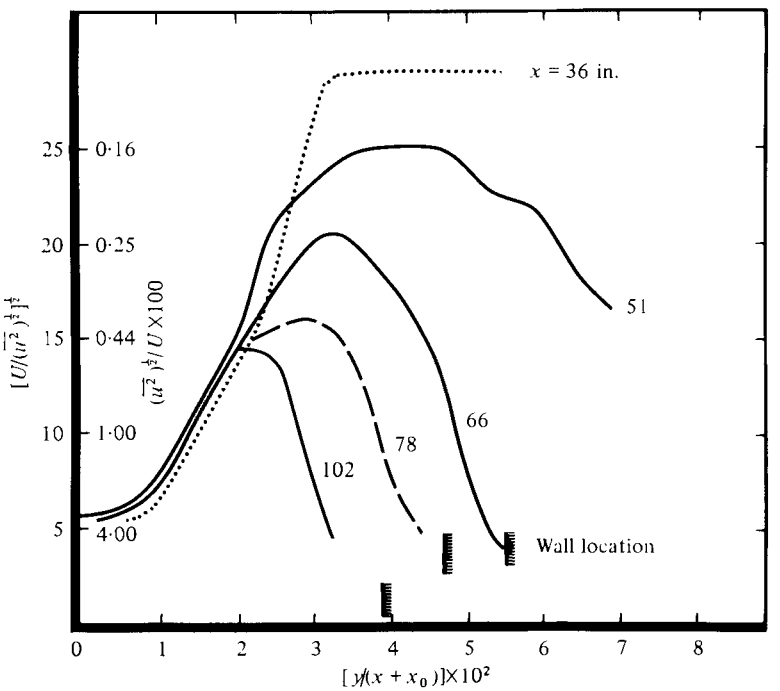

FIGURE 5. Fluctuation intensities from mixing layer and nearby boundary layer from tests II (*a*).

apparent turbulent intensity. It is convenient to plot the inverse of the intensity in describing this effect so that, as shown in figure 5, a maximum in $[U_1/(\overline{u^2})^{\frac{1}{2}}]^{\frac{1}{2}}$ represents the minimum intensity. The use of the variables in figure 5 avoids uncertainties in the value of y_I. In the furthest upstream measurements, a broad plateau of constant $U_1/(\overline{u^2})^{\frac{1}{2}}$ is present, equivalent to an intensity of about 0·12 %. Further down the tunnel, the plateau narrows to a maximum as the irrotational regions overlap. In all cases, however, there is a significant section for which

$$[U_1/(\overline{u^2})^{\frac{1}{2}}]^{\frac{1}{2}} \propto y/x + \text{constant}, \tag{7}$$

as suggested by Phillips for the irrotational region.

The extent to which the observed free-stream intensity variation can be thought of as a simple sum of two irrotational fields is demonstrated in figure 6, where, for $x = 102{\cdot}5$ in., the observed distribution is replotted from figure 5. Drawn through the curve describing the measurements are two straight lines whose form is like that of (7), each representing the irrotational field from one of the turbulent flows. If these fluctuations are instantaneously additive but not correlated, then one can easily show that

$$\overline{u^2} = \overline{u_1^2} + \overline{u_2^2}, \tag{8}$$

where u_1 and u_2 are the irrotational fluctuations due to each field and are represented by the mean lines 1 and 2 in figure 6. Several points calculated from these means lines and (8) are also shown in figure 6; they underestimate the observed curve slightly but represent the trend correctly. On the assumption that the irrotational field from the

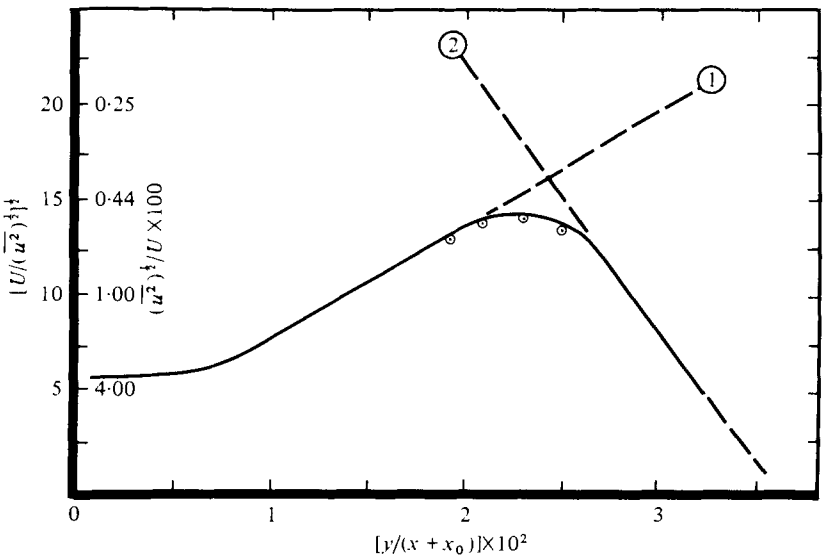

FIGURE 6. Details of fluctuation intensities in overlap region between mixing layer and nearby boundary layer; tests II(*a*), $x = 102$ in.

tunnel boundary layer is not influencing the mixing-layer characteristics appreciably, we have quoted the effective free-stream turbulence as between 0·1 % and 0·2 %, the minimum values present at the furthest upstream stations and evident on the 'plateaus' of figure 5.

Dean & Bradshaw (1976) have concluded that parallel shear layers in close proximity do not affect each other significantly for some distance, the turbulence fields 'time-sharing' the region between them. This is possible in the present case, although the fields, if irrotational, can co-exist as well, the velocities from each side being additive.

A second comment in connexion with this 'low turbulence' mixing layer is that a small vibration of the dividing plate had no effect on the rate of growth dL_0/dx or the stress distributions in the flow. The small (or order 0·01 in. or less) vibration of the plate would not have been noticed or mentioned had it not created flapping oscillations of the mixing layer which were very obvious in the correlation measurements described in the next section. Experiments in which the plane was oscillated artificially at other frequencies and higher amplitudes are also described in § 4.

A 'high turbulence' mixing layer was also investigated with the experimental arrangement in figure 2(*b*). Honeycombs ($\frac{3}{8}$ in. cell size, 6 in. deep) placed above and below the dividing plate introduced turbulence whose relative intensity was about 1 % in the lower-velocity stream and $1\frac{1}{2}$ % in the higher-velocity stream measured 43 in. downstream, then appeared to increase for reasons already discussed. Since the maximum longitudinal intensity in this flow, relative to local mean velocity, is about 5 %, the external intensity of around 1 % is not small by comparison. The velocity ratio in this case was 0·77, and results are designated as II(*b*) or 'high turbulence'.

The width of the mixing layer is plotted as L_0 *vs.* x in figure 7. The width grows linearly, as expected, perhaps with the exception of the last point. Because of this layer's greater size, the tunnel walls may have influenced the growth rate at this furthest downstream position. The maximum longitudinal intensity expressed as a

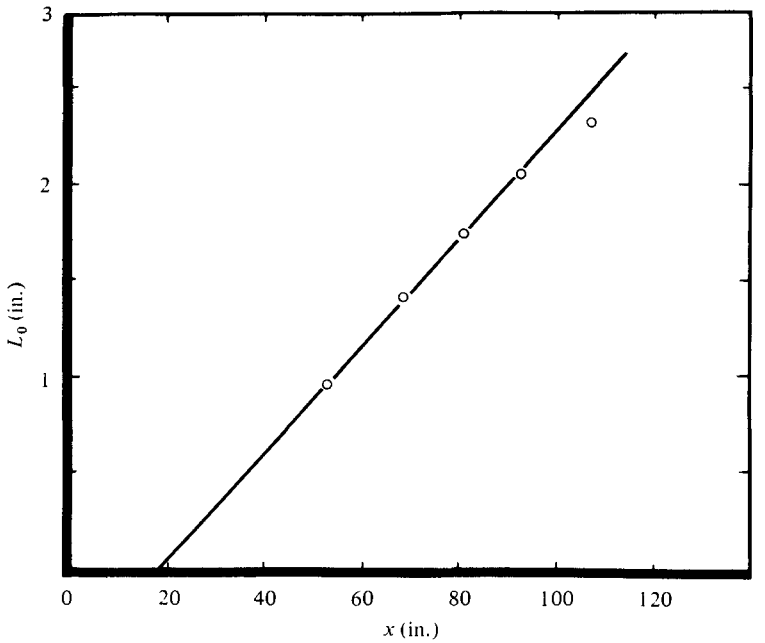

FIGURE 7. Mixing-layer width from tests II(*b*); $U_2/U_1 = 0{\cdot}77$.

fraction of U_0 varied from 0·237 upstream to 0·217 downstream, the mean value of 0·225 being shown in table 1. This layer appears also to be close to self-preservation; its virtual origin has moved downstream considerably compared with the 'low turbulence' case, perhaps owing to the honeycomb's inhibiting effect on the initial entrainment.

This mixing layer, in common with those measured by Pui, has a considerably higher growth rate than would be predicted from (4) and the Liepmann–Laufer growth rate for $U_2 = 0$. For a mixing layer of velocity ratio 0·77, this equation predicts a growth rate dL_0/dx of 0·021; the corresponding value of 0·029 observed in the experiments (see results II(*b*) in table 1) is about 40 % greater. The maximum longitudinal turbulence level, non-dimensionalized by U_0, is also much greater than that observed in the 'low turbulence' case. Apparently all Reynolds stresses increase by about the same proportion owing to the addition of external turbulence, since maximum shear stresses are proportional to the growth rate from (6). Only longitudinal intensities were measured directly in this case.

The results summarized in table 1 confirm the suggestion made by Patel, Rodi and others that the addition of small-scale free-stream turbulence increases mixing-layer growth rates. The turbulence levels in the flow and the flow 'constant' $\overline{uv}/U_0^2$ are also clearly increased. This helps to explain much of the scatter in these quantities noted by Rodi in his summary of data, particularly at high values of U_2/U_1, where sensitivity to free-stream turbulence would probably be greatest. It is not clear whether decreasing free-stream turbulence levels would always produce lower growth rates and intensities or whether a definitive low turbulence structure has been reached in these tests. The latter appears likely and extremely low free-stream turbulence levels are not of practical interest in any case.

4. Large-scale turbulent structures

In the 'low turbulence' mixing-layer (II*a*), experiments were made to measure some characteristics of the large-eddy structure in the well-developed region. It was decided that evidence of the largest structure could be obtained by time-delay cross-correlation measurements between normal hot wires located on opposite sides of the layer. Accordingly, two linearized hot wires were placed at the same x and z, one at $y_{0\cdot1}$ and the other at $y_{0\cdot9}$, a distance of 1·55 in. apart for $x = 68\cdot5$ in., where most of the measurements were made. The maximum velocity U_1 was 21 ft/s and $U_2/U_1 = 0\cdot83$.

As already mentioned, the cross-correlations with time delay first showed a very strong oscillation at about 29 Hz; autocorrelations also contained this frequency. This regular, repeated oscillation was initially construed as evidence of the Brown–Roshko structure. The 29 Hz frequency was, however, independent of tunnel speed and streamwise position and was finally traced to vibration in the structure (mainly arising from the counter-rotating fans driving the tunnel) which oscillated the splitter plate slightly. All evidence of the 29 Hz repeated oscillation was removed from the cross-correlation and autocorrelation signals by balancing the fans with care, separating them slightly from the rest of the tunnel structure and restraining the splitter plate with fine wires.

It appears likely that the vibrating splitter plate excited a standing acoustic wave whose frequency was dependent on the tunnel length and the local speed of sound but independent of the streamwise position and tunnel speed. The acoustic wave in turn created a flapping oscillation of the shear layer evident in the correlations. The overall tunnel length from inlet to outlet is about 21 ft, for which the half-wave resonance frequency based on an acoustic speed of 1120 ft/s is about 27 Hz, close enough to the observed value of 29 Hz to provide a plausible explanation.

To investigate the sensitivity of the shear layer to oscillations at other frequencies, an external frame was devised so that the splitter plate could be driven at various amplitudes and frequencies by a mechanical shaker located outside the tunnel. The cross-correlation already described, measured at a point 68½ in. downstream of the splitter-plate trailing edge, showed no evidence of regular oscillations unless the exciting frequency was close to a simple multiple of 29 Hz. At 29 Hz or its harmonic, large oscillating cross-correlations and oscillating autocorrelations again appeared, similar to those seen before. This evidence again supports the interpretation of the resonance as an acoustic wave not connected with the fundamentals of mixing-layer structure. These experiments did show, however, how sensitive the mixing layer is to external disturbances. Final measurements of mixing-layer growth and structure were made only when all air-conditioning fans in the laboratory were turned off and when all other external disturbances were minimized. Such precautions were necessary to obtain moderately steady results.

With the splitter plate fixed and all evidence of the acoustic wave removed, measurements of the large-eddy structure were taken. Cross-correlations at $x = 68\frac{1}{2}$ in. were again measured with linearized normal hot wires at the $y_{0\cdot1}$ and $y_{0\cdot9}$ points.

A large-eddy structure generated by the flow produced the cross-correlation with time delay shown in figure 8. This was not produced by initial instabilities of the laminar shear layer, as shown by experiments to be described later in this report. Autocorrelations and cross-correlations with the probes closer together were less

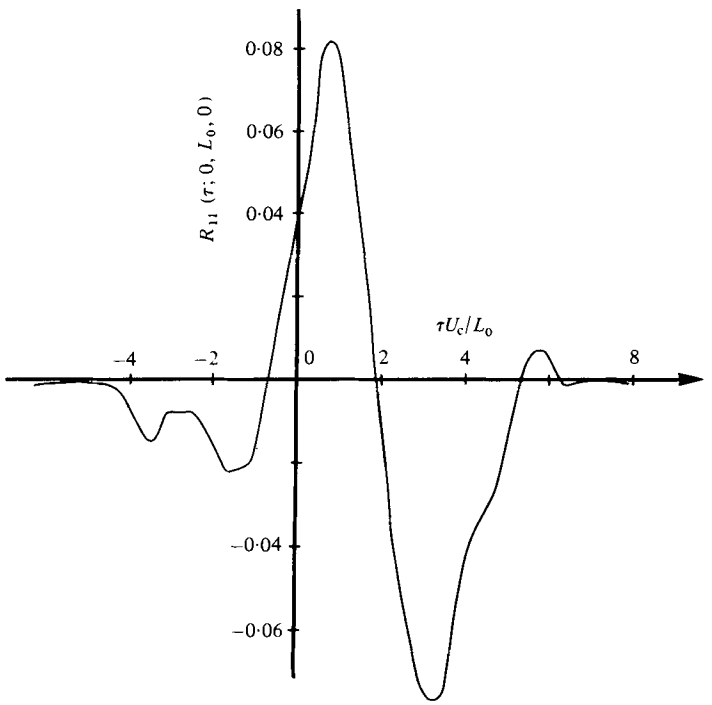

FIGURE 8. Cross-correlation with time delay; $x = 68{\cdot}5$ in., $\Delta z/L_0 = 0$.

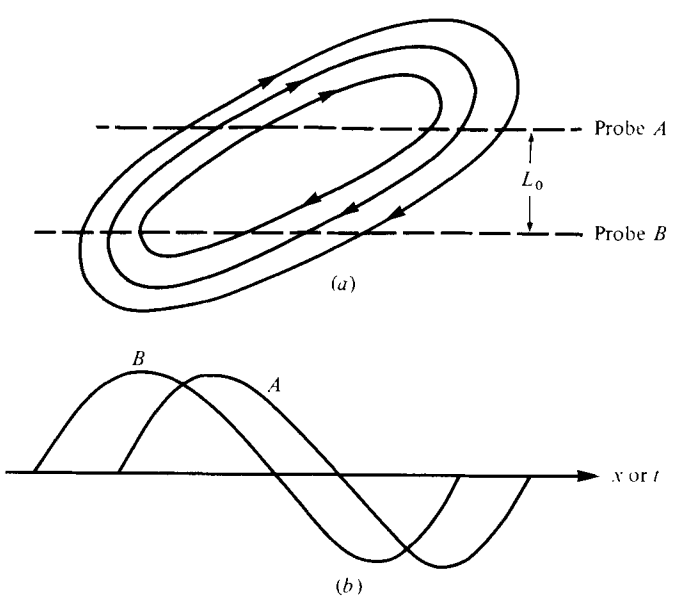

FIGURE 9. Possible large-eddy pattern causing correlation of figure 8. (*a*) Large-eddy streamlines. (*b*) Longitudinal velocities from large eddy seen by probes at levels A and B.

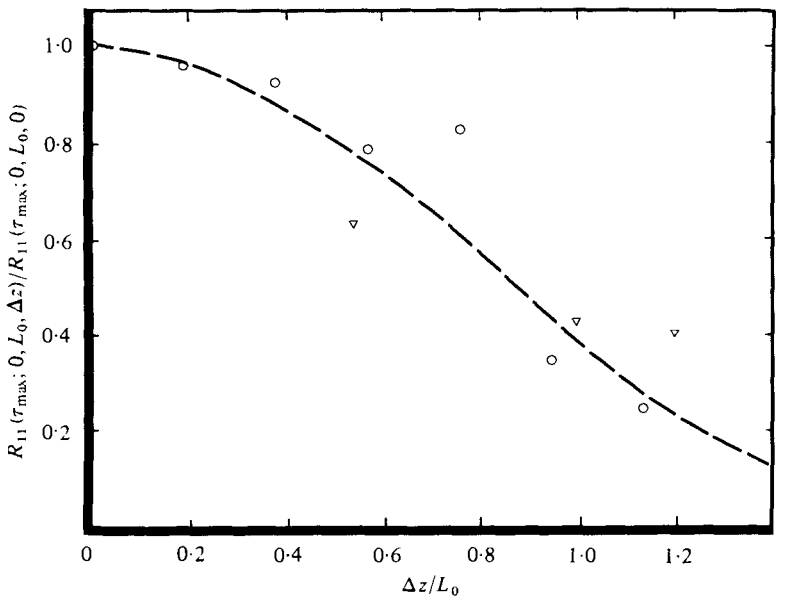

FIGURE 10. Maximum magnitude of cross-correlations. ⊙, run 1; ▽, run 2.

informative about the large-eddy structure, being much more influenced and in most cases dominated by smaller scales. That large differences can occur between large- and small-scale structures, particularly in convection speed and lateral correlation extent, is evident from the published measurements of Jones, Planchon & Hammersley (1973).

The cross-correlation plots obtained were not completely steady; this is not surprising since only a rather small part of the turbulent mixing-layer energy (itself rather weak in this case) is correlated across the distance L_0. Small disturbances to the flow, arising perhaps from disturbances in the room, which acted as the return circuit of the blower wind tunnel, changed the relative magnitudes in the correlation pattern. The overall shape remained clear however.

The correlation of figure 8, as do others taken, becomes essentially zero for a large positive or negative time delay, and therefore does not indicate a series of regular repeated structures.

It is interesting to speculate on the large-eddy structure which would produce the correlation of figure 8. The pattern is not unlike a simple cosine function of τ with frequency ω and phase lag τ_0, appearing for one complete cycle only. This shape can be produced by the correlation of two sinusoidal functions both of frequency ω but displaced from each other by a time τ_0. Because only large-scale motions will be correlated at all, the two sinusoidal functions represent only the velocity components (in the streamwise direction) of the largest eddies. One possible structure producing such sinusoidal fluctuations is sketched in figure 9, a velocity distribution not unlike those seen by Brown & Roshko (1974) and by Winant & Browand (1974). The wavelength of the structure in figure 9 can be estimated from the period of figure 8 as about six times the local thickness L_0 or, using (3), about 5·5 times the thickness l defined from the maximum velocity derivative. This is comparable to, but slightly larger than, the structure spacing observed by Dimotakis & Brown (1976), who quoted

$$3{\cdot}1 < \tau_0 U_c/l < 5{\cdot}0,$$

in the present notation. In all cases the convection speed U_c is assumed to be equal to $\frac{1}{2}(U_1 + U_2)$, the mean speed of the layer, an assumption made by Dimotakis & Brown on the basis of measurements by Jones *et al.* (1973).

The extent to which the observed large-eddy structure was two-dimensional was next investigated. For this the hot wire in the lower-velocity stream was moved laterally across the tunnel (in the z direction) while keeping the hot wires at the same spacing in the y direction, i.e. at the $y_{0\cdot1}$ and $y_{0\cdot9}$ points. The wires were maintained at the same streamwise position, both $68\frac{1}{2}$ in. from the splitter plate. As before, only contributions to the largest scales were correlated and the two-dimensionality of these large structures could be inferred from cross-correlations with time delay made at various lateral spacings Δz.

The results are summarized in figure 10, which shows the maximum amplitude of the negative peak in the cross-correlation for various values of Δz. Despite the scatter in these results, which is not surprising in view of the quantitative unsteadiness of the correlation already discussed, it is clear that the large structure has a length scale in the z direction which is of the order of L_0, which means that the scales in the y and z directions are comparable. This is in direct contrast to the results measured or implied in the results of Brown & Roshko (1974), Jones *et al.* (1973), Dimotakis & Brown (1976) and Oster *et al.* (1976), all of whom report large structures whose scale in the z direction is much larger than that in the y direction.

The results of figure 10 do not admit the possibility of a two-dimensional eddy skewed such that its axis is at some moderately small angle to the z axis. Such an eddy, if present, would change the time delay at which a maximum correlation is observed but would maintain the same (or a gradually reducing) maximum correlation for increased Δz.

Since it has been suggested (Bradshaw 1976) that the two-dimensional Brown–Roshko structures are a relic of the transition process in a laminar shear layer, the initial conditions near the plate in the present shear layer were next investigated to see whether normal transition is occurring in this case. For these experiments the splitter plate was held rigidly and the flow close to its trailing edge was studied with a single linearized normal hot wire.

The boundary layers above and below the plate appeared to be laminar and the wake formed just downstream of the plate displayed a very clear single frequency of about 460 Hz, plus higher harmonics. Further downstream the same fundamental frequency and harmonics were observed but were gradually submerged in broad-band fluctuations, disappearing entirely some 16 in. downstream of the plate. Mean velocity profiles measured 1·1 and 3·8 in. downstream of the plate contained a wake from the plate in the middle of the shear layer. This wake had disappeared from the mean velocity at $x = 16$ in.

These observations are all compatible with wake-type vortex shedding from the rear of the dividing plate. The Strouhal number found from the fundamental frequency (460 Hz), the mean velocity $\frac{1}{2}(U_1 + U_2)$ and the plate thickness (0·0625 in.) is 0·12. This value is in the expected range. No evidence of pairing, i.e. a reduction in frequency by a factor of two or three, was observed and other spectra downstream do not show evidence of a dominant frequency. This suggests that the energy in the large coherent structures discussed in the previous paragraphs is not sufficient to produce an identifiable peak in the spectra.

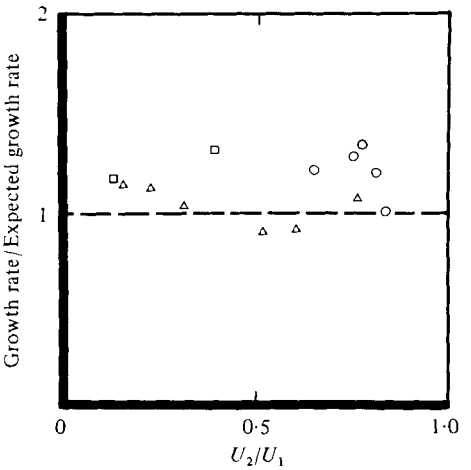

FIGURE 11. Comparison of selected growth rates. △, Spencer & Jones (1971); ⊡, Brown & Roshko (1974); ○, present tests I and II.

5. Concluding discussion

While the experiments described here confirm the idea that free-stream turbulence affects the growth rate of turbulent mixing layers, there is still not sufficient information to quantify this effect over the entire velocity-ratio range, nor is there much information available on the effect of the scale of the free-stream turbulence on this process. On the latter point, it seems clear that very large scales of free-stream turbulence will not affect growth rates or turbulence structures in the mixing layer itself; the acoustic wave inadvertently encountered in the present experiments is an example of a large disturbance having little or no effect on the growth rate.

The present experimental method of adding free-stream turbulence, by means of honeycomb flow straighteners, affects both the initial conditions, such as boundary layers on the splitter plate, and the free-stream turbulence simultaneously. The way in which initial conditions can affect the mixing-layer growth, as shown by Batt and by Oster *et al.*, needs clarification; it may be that the initial-condition effects observed by these workers include alterations in the free-stream turbulence near the mixing layer for some distance downstream. Certainly the present experiments show that mixing layers are very sensitive to external free-stream disturbances, but it is difficult to see how a mixing layer can be truly self-preserving if it continues to be affected by the details of its initial conditions. Local boundary conditions, on the other hand, can clearly affect the development of a self-preserving flow, so that it is possible to have a variety of nearly self-preserving mixing layers each with a different free-stream turbulence condition and growth rate but with the same mean velocity ratio.

From the present experiments and others reported previously, it appears that the two-dimensional structure observed by Brown & Roshko and others can be present only when a laminar mixing layer and a resonably normal transition region are present near the origin. The exact conditions under which the Brown–Roshko structure will appear and persist remain to be determined however. Chandrsuda *et al.* (1978) show that increasing small-scale turbulence introduced near the origin of the mixing layer, particularly on the low-velocity side, reduced the strength and persistence of the two-

dimensional pattern. Wygnanski & Oster (1979), on the other hand, have found that turbulence introduced on the high-velocity side does not always disrupt the two-dimensionality of the structures. In any case, the degree to which the large eddies are two-dimensional does not appear to affect the growth rate of the mixing layer significantly, so that this phenomenon, while visually startling, may not be of great importance.

Figure 11 summarizes measured growth rates from Spencer & Jones (1971), Brown & Roshko (1974) and the present experiments. In the first case (Spencer & Jones), later measurements reported by Jones *et al.* (1973) show that the large structures were strongly two-dimensional; Brown & Roshko's structures were also two-dimensional but those in the present experiments were not, at least in the case $U_2/U_1 = 0{\cdot}83$. The variation in the growth rates seen in this figure can be readily accounted for in terms of free-stream turbulence (about 0·1 % for Spencer & Jones, between 0·1 and 0·5 % for Brown & Roshko and between 0·12 and 1 % for the present experiments, whose details are reported in table 1). So far, there is no correlation between the presence of two-dimensionality and high or low growth rates, so that it seems reasonable to assume that the *effective* turbulent structure is the same in all cases, independent of both the velocity ratio *and* large-eddy two-dimensionality. The value chosen as a basis for comparison at $U_2 = 0$ in figure 11 is that reported by Liepmann & Laufer. A more complete comparison of growth rates reported by other workers is given by Rodi (1975).

The large-eddy structure sketched in figure 9 is certainly not the only one that could produce the correlation in figure 8, so that more measurements are necessary to refine and improve the suggestion inherent in the former figure. One structure, the double roller eddy suggested by Townsend (1976), is not compatible with the observed correlation however, unless the axes of the rollers are inclined over some part of their length to the y, x plane, as well as to the y, z plane (in present notation). The familiar stretching and energy-cascade concepts require a three-dimensional structure something like that sketched by Townsend, but such structures could co-exist with the other type of large eddy sketched in figure 9, whether in two- or three-dimensional form. It may be that different diagnostic tools such as visualization or the present cross-correlations with time delay merely identify different features of what we already know to be a very complicated flow.

The conclusions which can be drawn from the present experiments are summarized below.

(i) An increase in the small-scale free-stream turbulence intensity can influence the development of apparently self-preserving mixing layers, increasing the Reynolds stresses and growth rates significantly.

(ii) The growth rates of mixing layers formed between parallel streams with low turbulence are not incompatible with the constant-structure model proposed by Görtler and used by others; Reynolds-stress distributions (non-dimensionalized by local length and velocity scales) appear to be roughly independent of the velocity ratio of the streams forming the layer.

(iii) The large structures in a mixing layer are not necessarily two-dimensional. Measurements made in the present case, using cross-correlations with time delay, show that large-eddy scales are of similar magnitude in the two cross-stream directions, in direct contrast to a number of other published papers which report much larger

spanwise length scales. The absence of two-dimensionality in the large scales does not influence the growth rate or Reynolds stresses significantly however.

We are grateful to Mr L. Hoglund and Mr A. G. Dean for making some of the measurements described here. This work was supported by the N.R.C. (Canada) under Grant Number A4308. A preliminary version of this work was presented at the 6th Canadian Congress of Applied Mechanics (1977).

REFERENCES

BATT, R. G. 1975 Some measurements on the effect of tripping the two-dimensional shear layer. *A.I.A.A. J.* **13**, 247–248.

BRADSHAW, P. 1976 Turbulence. In *Topics in Applied Physics* vol. 12, (ed. P. Bradshaw), pp. 41–43. Springer.

BROWN, G. L. & ROSHKO, A. 1974 On density effects and large structure in turbulent mixing layers. *J. Fluid Mech.* **64**, 775–816.

CHAMPAGNE, F. H., PAO, Y. H. & WYGNANSKI, I. J. 1976 On the two-dimensional mixing region. *J. Fluid Mech.* **74**, 209–250.

CHANDRSUDA, C., MEHTA, R. D., WEIR, A. D. & BRADSHAW, P. 1978 Effect of free-stream turbulence on large structure in turbulent mixing layers. *J. Fluid Mech.* **85**, 693–704.

DEAN, R. B. & BRADSHAW, P. 1976 Measurements of interacting turbulent shear layers in a duct. *J. Fluid Mech.* **78**, 641–676.

DIMOTAKIS, P. E. & BROWN, G. L. 1976 The mixing layer at high Reynolds number: large structure dynamics and entrainment. *J. Fluid Mech.* **78**, 535–560.

JONES, B. G., PLANCHON, H. P. & HAMMERSLEY, R. J. 1973 Turbulent correlation measurements in a two-stream mixing layer. *A.I.A.A. J.* **11**, 1146–1150.

LIEPMANN, H. W. & LAUFER, J. 1947 Investigation of free turbulent mixing. *N.A.C.A. Tech. Note* no. 1257.

OSTER, D., WYGNANSKI, I. & FIEDLER, H. 1976 Some preliminary observations on the effect of initial conditions on the structure of the two-dimensional turbulent mixing layer. *SQUID Symp. Virginia.*

PATEL, R. P. 1973 An experimental study of a plane mixing layer. *A.I.A.A. J.* **11**, 67–71.

PHILLIPS, O. M. 1955 The irrotational motion outside a free turbulent boundary. *Proc. Camb. Phil. Soc.* **51**, 220–229.

PUI, N. K. 1969 The plane mixing region between parallel streams. M.A. Sc. thesis, University of British Columbia.

RODI, W. 1975 A review of experimental data of uniform density free turbulent boundary layers. In *Studies in Convection*, vol. 1 (ed. B. Launder), pp. 79–166. Academic Press.

ROSHKO, A. 1976 Structure of turbulent shear flows: a new look. *A.I.A.A. J.* **14**, 1349–1357.

SABIN, C. M. 1965 An analytical and experimental study of the plane, incompressible, turbulent shear layer with arbitrary velocity ratio and pressure gradient. *Trans. A.S.M.E., Basic Engng* **87**, 421–428.

SCHLICHTING, H. 1969 *Boundary Layer Theory*, 4th edn. McGraw-Hill.

SPENCER, B. W. & JONES, B. G. 1971 Statistical investigation of pressure and velocity fields in the turbulent two-stream mixing layer. *A.I.A.A. Paper no.* 71–613.

TOWNSEND, A. A. 1976 *The Structure of Turbulent shear Flow*, 2nd edn. Cambridge University Press.

WINANT, C. D. & BROWAND, F. K. 1974 Vortex pairing: the mechanism of turbulent mixing-layer growth at moderate Reynolds number. *J. Fluid Mech.* **63**, 237–255.

WYGNANSKI, I. & FIEDLER, H. E. 1970 The two-dimensional mixing region. *J. Fluid Mech.* **41**, 327–362.

WYGNANSKI, I. & OSTER, D. 1979 On the perseverence of a quasi two-dimensional eddy structure in a turbulent mixing layer. Submitted to *J. Fluid Mech.*